JACS
JOURNAL OF THE AMERICAN CHEMICAL SOCIETY
pubs.acs.org/JACS
Article

Intersegment Transfer and the Dynamical Architecture of Fis Protein−DNA Multimer Complexes

Xun Chen,* Shikai Jin, Cheng-Han Liu, Yaakov Levy,* Min-Yeh Tsai,* and Peter G. Wolynes*

Cite This: J. Am. Chem. Soc. 2025, 147, 30277−30286

ABSTRACT: Gene regulation often entails a cooperative dynamic interplay among several protein molecules and several distinct DNA segments. Intersegment transfer of the Fis protein stimulates DNA inversion during DNA recombination. Individual DNA segments have been found to facilitate the dissociation of Fis proteins already bound to DNA and also allow for the transfer of the Fis between segments. Here, we use the hybrid coarse-grained AWSEM/3SPN.2C model to simulate the Fis protein intersegment transfer and explore its mechanism. We show that entropic effects within the Fis protein−DNA complex dictate the transfer pathway through specific structural configurations, involving specific grooves and consequent orientation constraints on the DNA segments. Multiple copies of the Fis protein facilitate intersegment transfer, explaining how changes in protein−DNA stoichiometry and concentration influence how the Fis−DNA complex architecture is established. This orientational dependence indicates that the assembly of the Fis−DNA complex mimics the interlocking of screws, functioning as a molecular machine that may couple to DNA supercoiling and torsional stress in the DNA generated by motor proteins, thus offering a potential regulatory mechanism for chromosomal organization and gene expression.

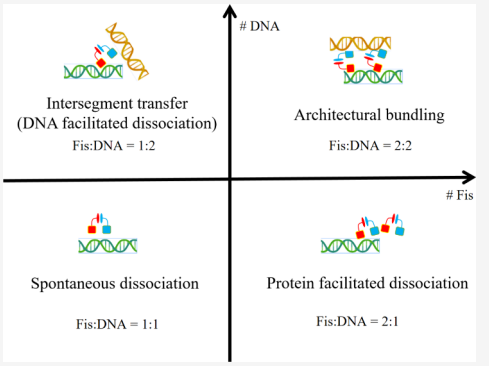

1. INTRODUCTION

The regulation of gene expression often involves complexes of multiple protein molecules and often multiple DNA segments containing distinct genomic information.[1,2] A well-studied example of the role of such complexes in regulation involves the Fis protein.[3,4] Fis (the factor for inversion stimulation) is found in E. coli, often described as a homodimeric DNA-bending protein or as "histone-like" or "nucleoid-associated" protein.[5−8] Fis protein was discovered in the regulation of DNA inversion where it was found to stimulate the Hin site-specific DNA recombinase of Salmonella.[9−12] Fis has a multitude of activities, including the activation of rRNA and tRNA transcription[13] as well as direct DNA replication[14] and the repression of its own synthesis.[8] Which of these activities prevails depends on the concentration of Fis, which varies dramatically under different growth conditions during the life cycle.[15−18] This complexity implies that Fis's functions depend on different complexes of differing molecularity.

The association, dissociation, and reassociation of Fis protein molecules must all be involved in the way Fis carries out these activities that depend on protein stoichiometry. Experiments show that not only Fis itself but also other biomolecules such as HU protein molecules and soluble DNA segments can catalyze the dissociation and reassociation of Fis protein already bound to a single DNA.[8,15,19,20] The dissociation rate of bound Fis protein increases as the concentration of these partners increases.[14,18] The facilitated dissociation of Fis protein is made possible by its dimeric nature,[21] which allows it to remain in contact with DNA without having both domains simultaneously participating. Facilitated dissociation arises when the partially bound Fis protein interacts with other Fis protein molecules[8] or other DNA segments[18] as well as with HU protein molecules.[22] Analogous phenomena have been observed in the behavior of a range of protein−DNA assemblies, including the interaction of HMGC (eukaryotic high-mobility)[23] and CueR (copper efflux regulator).[24] Doubtless, such multiprotein DNA associations are present in a host of biological functions. The "direct transfer" of Fis protein molecules between distinct DNA segments, so-called intersegment transfer, has been studied with magnetic tweezers.[16−18] The mechanism of this process is the focus of the present paper. Fis protein is not unique in its capability to participate in such intersegment transfer. Intersegment transfer processes have been observed for a wide variety of DNA-binding proteins such as the Lac repressor.[25,26] Intersegment transfer also can take place between single-strand DNA segments and features in the mechanisms of action of RecA and SSB.[27,28] Using the energy

Received: June 2, 2025
Revised: July 30, 2025
Accepted: July 30, 2025
Published: August 5, 2025

https://doi.org/10.1021/jacs.5c09262
J. Am. Chem. Soc. 2025, 147, 30277−30286

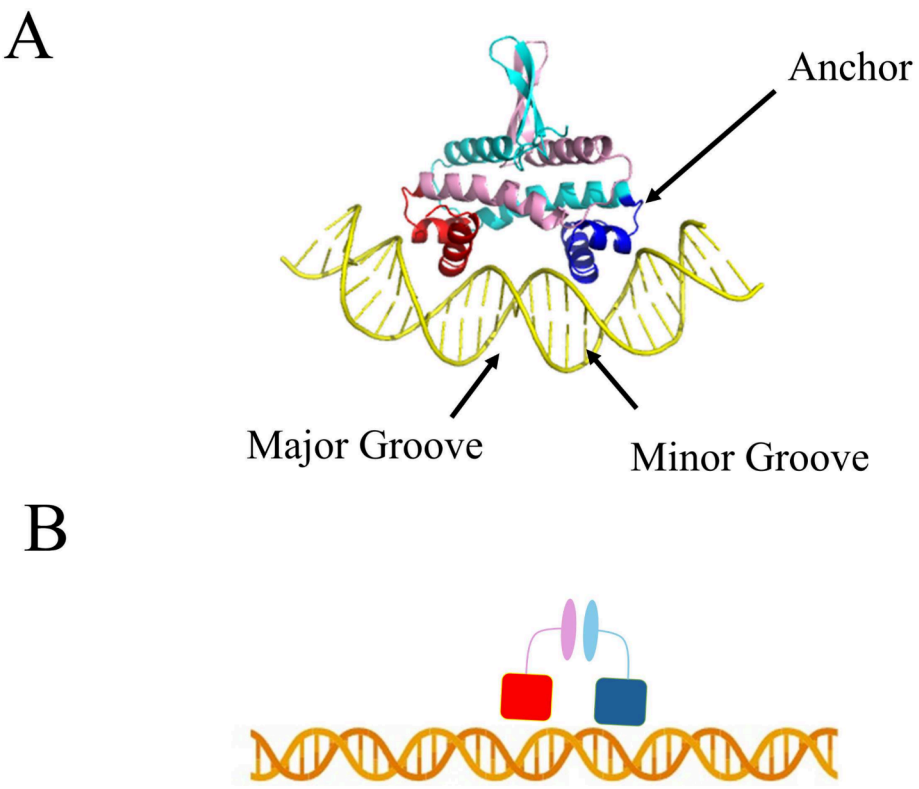

Figure 1. A) The schematic illustration of the complex between Fis protein and a single DNA. The Fis molecule and the DNA molecule are shown in the cartoon. The Fis molecule is a homodimer with two individual chains (chain A and chain B). In chain A, the DNA binding domain (the anchor part) is colored red; residues other than the anchor in the chain are colored pink. Similarly, in chain B, the anchor part is colored blue; residues other than the anchor in the chain are colored cyan. The DNA molecule is colored yellow. B) A schematic version of the Fis protein−DNA complex is shown.

landscape theory along with coarse-grained modeling, Tsai et al. explained the concentration dependence of Fis dissociation from individual DNA segments.[19] Their study distinguished a cooperative dissociation pathway from facilitated dissociation.[20] Here, we will further explore the intersegment transfer behavior of the Fis protein, which involves Fis interacting with distinct DNA segments.

We computationally survey the binding landscapes of Fis protein with multiple DNA segments using the hybrid coarse-grained AWSEM/3SPN.2C model.[19,29] This model has proven itself capable of studying diverse protein−DNA systems and processes, including the molecular stripping of the NFκB−DNA complex[30] by IκB, a key process in the immune response, the facilitated dissociation and cooperative dissociation of Fis from individual DNA segments,[19,20] and the recognition of DNA signals by PU.1 via indirect readout.[31] The sequence specificity of Fis protein does not require DNA to open and expose specific bases but rather mainly comes from indirect readout of DNA elastic properties,[18] suggesting that like those previous studied systems the interaction between Fis protein molecules and DNA segments mainly comes from the electrostatic interactions which can be modeled by the Debye−Hückel potential. Using this coarse-grained model along with the weighted histogram method (WHAM) to construct free-energy profiles that allow us to calculate rate constants using Kramers' theory, these predictions lead to predicted rates that agree well with experimental data. Using these free-energy surfaces, we examine the structural details of the key Fis protein−DNA intermediate complexes, focusing on the anchor and nonanchor regions of the Fis protein and their specific interactions with the major and minor grooves of DNA. This interplay determines how the kinetics of intersegment transfer depends on the relative orientations of the two DNA segments. The simulations show how an additional Fis protein molecule further facilitates dissociation and alters the transfer pathway through structures having complex architectures, explaining how changes in the Fis protein/DNA concentration ratio influence intersegment transfer.

2. RESULTS

2.1. Energy Landscape of the Fis Intersegment Transfer. Fis protein molecules may dissociate individually from DNA but also may be pulled off by other molecules. This process has been termed a facilitated or cooperative mechanism of dissociation.[19,20] We first focused on tracking the interactions between one Fis protein with multiple DNA segments. As illustrated in Figure 1, the Fis protein remains attached to the major groove of the DNA through its anchors, which are colored blue or red in the figure. Using the hybrid coarse-grained AWSEM/3SPN.2C model, we first investigated the binding free-energy profiles of the Fis protein with two DNA segments. Figure 2 (A) presents a free-energy profile constructed by simultaneously projecting the free energy onto the magnitude of electrostatic interactions between chain A of the Fis protein and segment DNA1 and the magnitude of electrostatic interaction between chain B of the Fis protein and segment DNA2. This pair of selected progress coordinates allows us to pick apart the correlation between the binding of each chain and the respective DNA segments. It is important to note that since both chains of the Fis protein are nearly

https://doi.org/10.1021/jacs.5c09262
J. Am. Chem. Soc. 2025, 147, 30277−30286

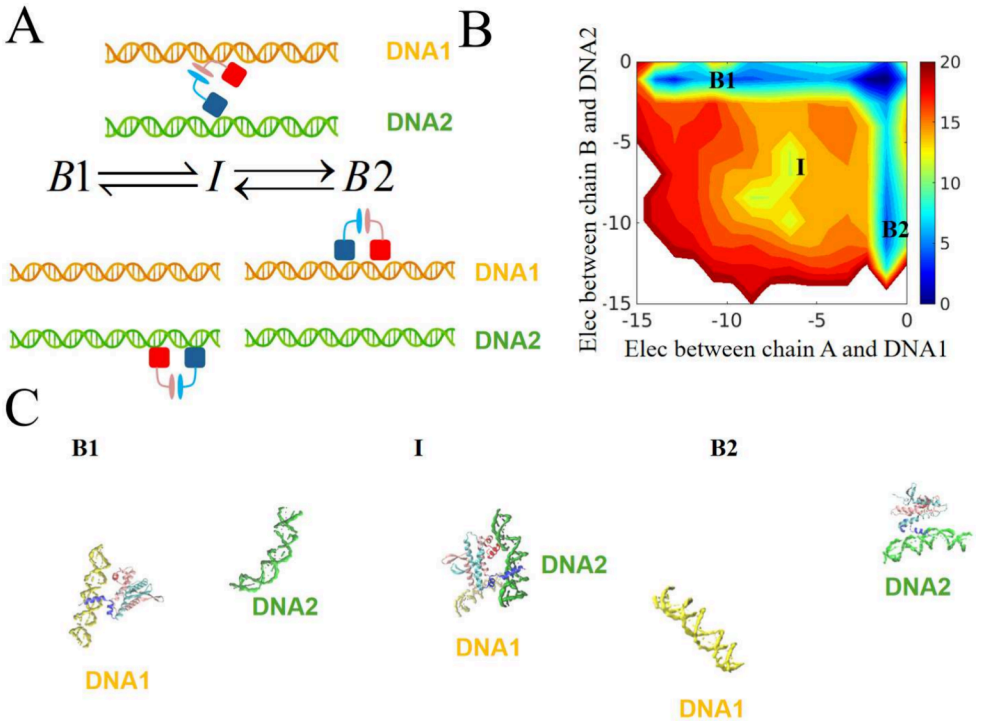

Figure 2. Kinetic pathway of intersegment transfer of the Fis molecule from DNA is visualized and shown. A) The sequential process of intersegment transfer. B) Two-dimensional free-energy profiles for Fis protein and DNA systems using the electrostatic interactions between chain A of Fis and DNA1 and the electrostatic interaction between chain B of Fis and DNA2. C) The representative structures labeled in the corresponding free-energy basin of B). The Fis protein is shown using a cartoon style, as depicted in Figure 1. DNAs are shown using surface style, where DNA1 is colored yellow while DNA2 is colored green.

identical and the two DNA molecules are chosen to have an identical sequence in the simulations, the free-energy surface is nearly symmetric along the diagonal, where multiple basins can be identified. These basins represent distinct architectures of protein−DNA co-complexes populated during the Fis intersegment transfer process.

The two deep basins, labeled B1 and B2, represent fully bound states. In these states, the two individual chains A and B each contribute approximately −10 kcal/mol of electrostatic interaction energy with DNA1 and DNA2, respectively. These basins correspond to the states where both chains are bound to the same DNA. Interestingly, we can identify an additional basin (I), in which these interactions are weaker but significant, suggesting the presence of an intermediate state during the transfer. Fis protein induces bending of DNA and significantly enhances fluctuations in local bending angles.

The calculated free-energy surface results suggest an intersegment transfer mechanism in which the Fis molecule moves between the two DNA strands in a stepwise manner. Initially, the fully bound Fis−DNA complex first undergoes partial dissociation in which one of the two anchors detaches from DNA2, which can then directly interact with the other DNA segment (DNA1). This divalent interaction of the Fis molecule thus creates an intermediate co-complex, the DNA1:Fis:DNA2 configuration, referred to as intermediate (I). During this transfer process, there is a shift in the strength of electrostatic interactions between the binding anchors and the DNA, compared to what happens when both parts of the Fis molecule are fully bound. This stepwise mechanism aligns with experimental observations, where competing DNA molecules facilitate the dissociation of the Fis protein from DNA.[18] The representative structures of these species identified from the free-energy profile in Figure 2(C) illustrate the intersegment transfer process in greater detail. The corresponding kinetic pathway is shown in Figure 2(B). We discuss the consistency of this model with experiments in the following section.

2.2. Architectural and Groove-Specific Roles of Fis Protein−DNA Complexes in Modulating Intersegment Transfer Pathways: Parallel vs Orthogonal DNA Orientations. In addition to using the magnitude of electrostatic interactions, we can pinpoint the interactions between the two Fis protein anchors and the DNA by monitoring position-dependent contacts at the Fis−DNA binding interface. We classified the specific protein−DNA contacts (Cbeta-phosphate < 9.5Å) into those made with the major grooves and those made with the minor grooves as well as the total number of protein−DNA interactions throughout the simulations. In addition to simulations where the DNA segments are free to rotate, we also performed two sets of simulations that constrained the two DNA molecules to be exactly either parallel or orthogonal to each other. This comparative approach allows us to evaluate the effects of the relative orientation of the DNA molecules on the intersegment transfer mechanism.

Our previous simulation work suggests that protein−DNA binding specificity involves an indirect readout mechanism,[31] driven by charge density coupled with DNA local bending. At this level of description, the most obvious intrinsic structural features of the DNA are the major and the minor grooves, which turn out to play distinct roles due to their differing local charge density profiles. To investigate this, we constructed a series of free-energy surfaces to examine the relationship

https://doi.org/10.1021/jacs.5c09262
J. Am. Chem. Soc. 2025, 147, 30277−30286

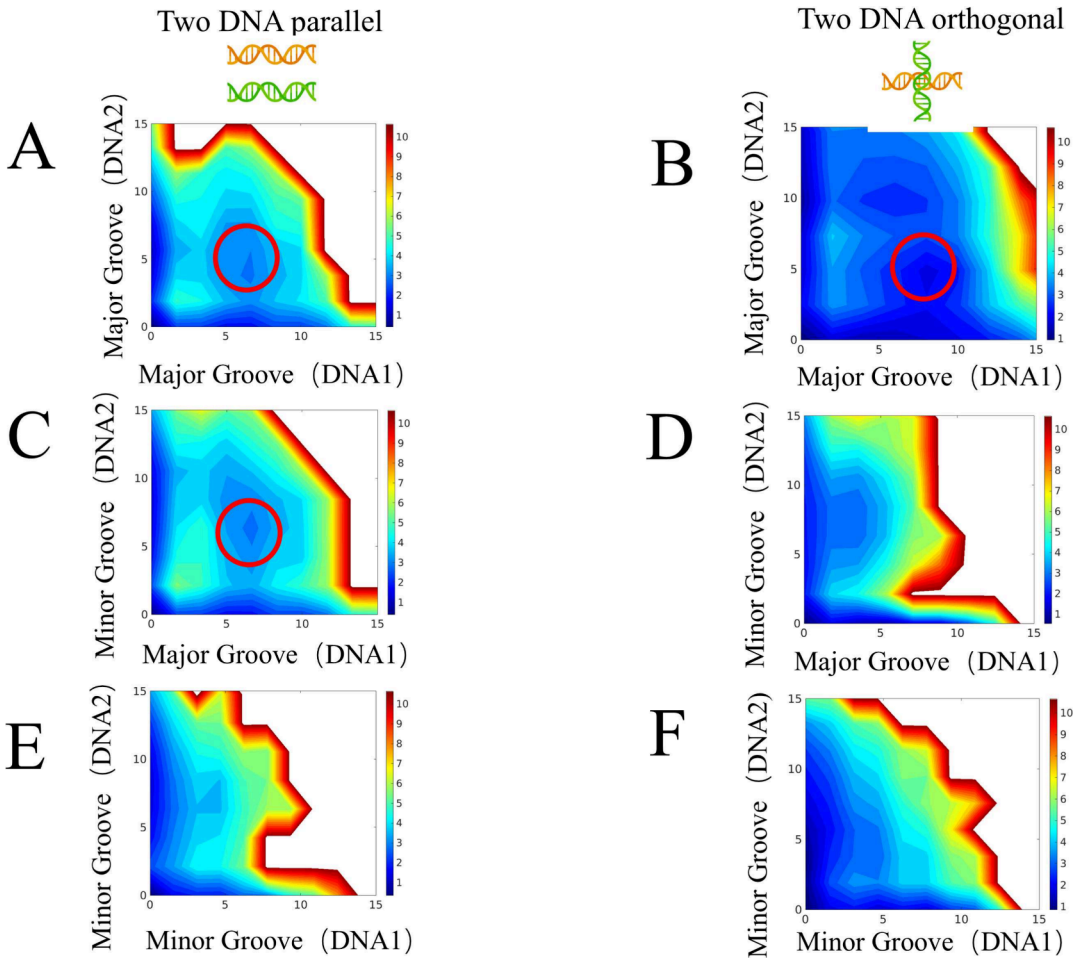

Figure 3. Two-dimensional free-energy profile of two parallel DNAs (A, C, E) shown as a function of the number of A) contacts formed between the anchor of chain A and the major groove of DNA1 and contacts formed between the anchor of chain B and the major groove of DNA2. C) Contacts formed between the anchor of chain A and the major groove of DNA1 and the contacts formed between the anchor of chain B and the minor groove of DNA2. E) Contacts formed between the anchor of chain A and the minor groove of DNA1 and the contacts formed between the anchor of chain B and the minor groove of DNA2. The two-dimensional free-energy profile of two orthogonal DNAs (B, D, F) is shown as a function of the number of B) contacts formed between the anchor of chain A and the major groove of DNA1 and the contacts formed between the anchor of chain B and the major groove of DNA2. D) Contacts formed between the anchor of chain A and the major groove of DNA1 and the contacts formed between the anchor of chain B and the minor groove of DNA2. F) Contacts formed between the anchor of chain A and the minor groove of DNA1 and the contacts formed between the anchor of chain B and the minor groove of DNA2.

between these grooves and the specific contacts they form in the intermediates as one varies the relative DNA orientation.

Initially, we constructed free-energy profiles based on the contacts between the anchor parts of the Fis protein and the distinct grooves of DNA molecules, considering varying relative orientations of the DNAs. Clear intermediate states, which are now identified by specific contacts within the major grooves of both DNAs, were observed in the free-energy profiles regardless of whether the DNAs were fixed in parallel or orthogonal configurations, as shown in Figure 3(A,B). The profiles indicate that the major grooves are the primary channel for intersegment transfer, regardless of the DNA orientation. Next, we investigated the intermediate states by examining specific contacts between the major and minor grooves. The intermediates were quantified through contacts between the anchor of chain A and the major groove of DNA1 and between the anchor of chain B and the minor groove of DNA2. This intermediate state persisted when the two DNAs were oriented in parallel but disappeared when the two DNAs were orthogonal, as illustrated in Figure 3(C,D). The free-energy surface for contacts involved in minor groove-to-minor groove interactions, as depicted in Figure 3(E,F), reveals no intermediates regardless of the relative orientation of the DNAs. Clearly, the relative orientation of the DNAs significantly influences the intersegment transfer mechanism.

Given the directionality of DNA sequences, one wonders whether DNA orientation creates distinct groove-interaction patterns that are different for binding to the 5′ to 3′ and the 3′ to 5′ directions. To explore this, we constructed a free-energy profile based on the number of contacts formed between chain A of the Fis protein and DNA1 and between chain B of the Fis protein and DNA2 when the DNAs are oriented antiparallel (Figure S3(A)). In this profile, we see that intersegment transfer occurs through partially bound intermediate species. These intermediates symmetrically bind to both DNAs, as indicated by consistent contact numbers with each DNA molecule. This profile is consistent with the electrostatic-based free-energy profile shown in Figure 2(A). The similar behavior of these intermediates in both parallel and antiparallel orientations of the DNAs further underscores the consistent

https://doi.org/10.1021/jacs.5c09262
J. Am. Chem. Soc. 2025, 147, 30277−30286

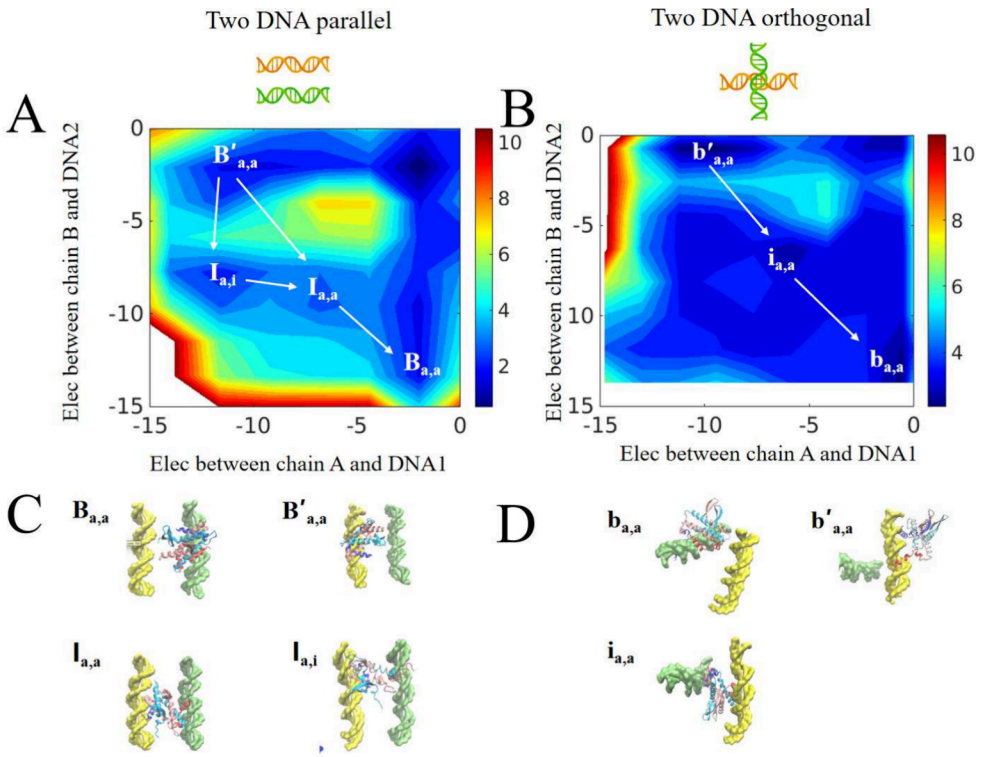

Figure 4. Kinetic pathways for intersegment transfer of the Fis molecule from DNAs that align parallel and orthogonal are compared. A) The two-dimensional free-energy profile using the electrostatics between chain A of the protein and DNA1 and the electrostatics between chain B of the protein and DNA2 when the two DNAs are parallel. B) The two-dimensional free-energy profile using the electrostatics between chain A of the protein and DNA1 and the electrostatics between chain B of the protein and DNA2 when the two DNAs are orthogonal. C) The representative structures in individual basins (labeled $B_{a,a}$, $B'_{a,a}$, $I_{a,a}$, and $I_{a,i}$ shown in A) are shown. B/b and I/i represent the bound and intermediate states of the Fis−DNA co-complex, respectively. Capital letters "B" and "I" denote the parallel orientation, while lowercase letters "b" and "i" denote the orthogonal orientation. The subscript indicates the type of anchor insertion: "a" for the major groove and "i" for the minor groove. $B_{a,a}$ and $B'_{a,a}$ refer to Fis's bound states where both anchors are inserted into the major grooves of DNA1 and DNA2, respectively. $I_{a,a}$ and $I_{a,i}$ refer to Fis's intermediate states where anchor B is inserted into DNA2's major groove while anchor A is inserted into DNA1's minor groove and major groove, respectively. D) The representative structures in individual basins (labeled $b_{a,a}$, $b'_{a,a}$, and $i_{a,a}$ in part B) are shown. $b_{a,a}$ and $b'_{a,a}$ refer to Fis's bound states where both anchors are inserted into the major grooves of DNA1 and DNA2, respectively. $i_{a,a}$ refer to Fis's intermediate state where anchor B is inserted into DNA2's major groove while anchor A is inserted into DNA1's major groove. Note that the Fis protein is shown in cartoon style. Anchor A of the Fis molecule (chain A) is colored red, while the chain's other parts are colored pink. Anchor B of the Fis molecule (chain B) is colored blue, while the chain's other parts are colored cyan. The DNA molecules are shown in quicksurf, where DNA1 is colored yellow while DNA2 is colored green.

influence of the DNA orientation on the intersegment transfer process.

The simulations reveal a wide variety of protein−DNA binding complexes, including some architectures in which the usually nonbinding parts of the protein engage in seemingly random interactions with the DNA molecules. The intersegment transfer intermediate, however, persists in the free-energy profile when one solely considers the anchors of the Fis protein (Figure S3(C)), but these intermediates disappear when only the nonanchor parts of the protein are used to monitor proximity (Figure S3(E)). Similar behaviors were seen in the simulations where the relative orientation of DNAs is restricted to orthogonal configurations (Figure S4(B,D,F)). These findings collectively suggest that the anchor regions of the Fis protein play the central role in the intersegment transfer process while the nonanchor parts of the Fis protein are essentially bystanders.

2.3. Orientational Role of the Fis Protein−DNA Complex in Modulating Kinetic Pathways of Intersegment Transfer. To further investigate the influence of the two DNAs' relative orientation, we constructed free-energy profiles based on the electrostatic interactions between chain A of the Fis protein and the DNA1 segment and chain B of the Fis protein with the DNA2 segment. As depicted in Figure 4(A), in addition to stable binding states ($B_{a,a}$ and $B'_{a,a}$ represent the Fis protein fully bound to the major grooves of DNA1 and DNA2, respectively, with the "prime" symbol distinguishing between the two DNA molecules; capital letters B/I denote states in the context of the DNA molecules in parallel orientation while lowercase letters b/i denote states in the orthogonal orientation), we observed two intermediates ($I_{a,a}$ refers to Fis binding DNA1's major groove and DNA2's major groove; $I_{a,i}$ refers to Fis binding DNA1's major groove and DNA2's minor groove) on the free-energy surface. Figure 4(C) shows that the intermediate ($I_{a,a}$), characterized by similar electrostatic energies of interaction with the two different DNAs, acts as a major−major groove species. In contrast, the intermediate ($I_{a,i}$), which displays different electrostatics with the two different DNA segments, acts as a major−minor groove species. Compared to the major−minor groove species, the weaker electrostatic interactions and the higher free energy of the major−major groove species suggest that they are energetically and thermodynamically unfavorable.

https://doi.org/10.1021/jacs.5c09262
J. Am. Chem. Soc. 2025, 147, 30277−30286

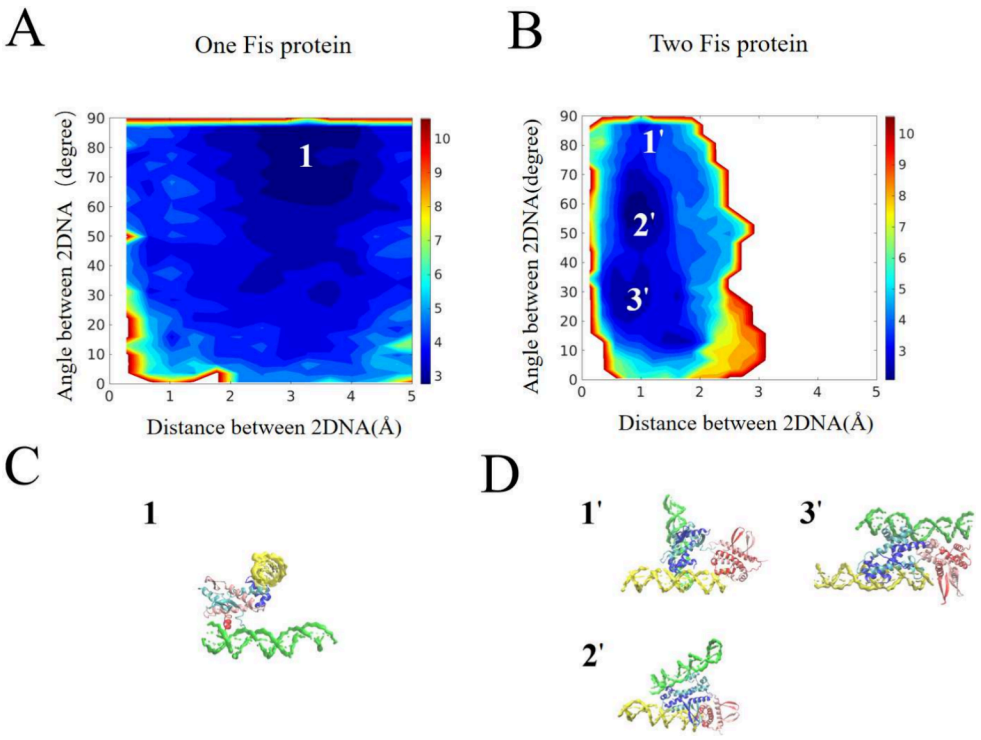

Figure 5. Distinct orientational effects on the two DNA molecules are observed with varying stoichiometries of Fis molecules. A) Two-dimensional free-energy profile showing the angle between the two DNA molecules and the distance between their centers of mass in a single Fis protein system. The free-energy surface is broad, with the major population ("1") indicating an angle close to orthogonal. B) Two-dimensional free-energy profile showing the angle between the two DNA molecules and the distance between their centers of mass in a dual Fis protein system. The free-energy surface is more constrained yet exhibits a greater diversity in orientation. The orthogonal configuration, now labeled as 1′, is less populated compared to 2′ and 3′, which correspond to intermediate angles (50−60°) and a nearly parallel configuration, respectively. C) Representative structures of each basin in the single Fis protein system shown in A: The Fis protein is depicted as a cartoon. Anchor A of chain A is colored red, with the remaining parts of chain A in pink. Anchor B of chain B is colored blue, with the remaining parts of chain B in cyan. DNA1 is shown in quicksurf and colored yellow, while DNA2 is colored green. D) Representative structures of each basin in the dual Fis protein system shown in B: The two Fis proteins are depicted as cartoons. The anchor of Fis1 is colored red, with the remaining parts of Fis1 in pink. The anchor of Fis2 is colored blue, with the remaining parts of Fis2 in cyan. DNA1 is shown in quicksurf and colored yellow, while DNA2 is colored green.

Moreover, the barrier between the major−minor groove intermediate and fully binding states is higher than the barrier between the major−minor groove intermediate and the major−major groove intermediate and the barrier between the major−major groove intermediate and fully binding states. This suggests that the major−minor groove intermediate is more likely to transition to a major−major groove intermediate before completing the transfer rather than transferring directly. Notably, the major−major intermediate is relatively stable in the orthogonal configuration of the two DNAs, whereas it is unstable in the parallel configuration. In the parallel configuration, the major−minor intermediate helps to bridge the free-energy gap between the fully bound state and the major−major intermediate, a gap that is negligible in the orthogonal configuration.

We see that there are two potential pathways for the intersegment transfer when the two DNAs are parallel: either through the major−major groove intermediate or through the major−minor groove intermediate, followed by a transition to the major−major groove intermediate, as shown in Figures S8 and S9. In contrast, when the two DNAs are orthogonal, only the pathway involving the major−major groove intermediate exists, as illustrated in Figure 4(B,D). These observations underscore how the architecture of the Fis protein−DNA complex significantly influences the kinetic pathways of intersegment transfer.

To further validate our hypothesis, we analyzed the DNA rotation angle (θ_1/θ_2) to assess the orientational behavior of the two DNA molecules within the protein−DNA complex. The rotation angles of DNA1 and DNA2 exhibit a highly synchronized relationship, suggesting that the Fis protein simultaneously engages with both DNAs at their grooves, facilitating the screw-like motion of the two DNA segments. This Fis-mediated screw-like motion of the two DNA segments occurs regardless of whether they are oriented parallel or orthogonal. This Fis-mediated screw-like motion of the DNA appears consistent with the mechanical constraints observed during site-specific recombination, where DNA supercoiling cooperatively regulates the rotation of the Hin subunit.[10] The screw-like motion of the DNA segments is more pronounced in the parallel configuration than in the orthogonal configuration, indicating that the intermediate state is trapped in the parallel arrangement (a low-entropy state). This observation supports the conclusion that intersegment transfer is less favorable in the parallel configuration, consistent with the higher free-energy barriers observed in the parallel case between the intermediate and fully bound states in the parallel mode of approach. The significance of DNA orientation in the intersegment transfer process is further underscored, with the orthogonal configuration being more conducive to Fis protein function. These findings, illustrated in Figures S5 and S10,

https://doi.org/10.1021/jacs.5c09262
J. Am. Chem. Soc. 2025, 147, 30277−30286

align with the proposed pathways for the intersegment transfer process.

2.4. Influence of Complex Stoichiometry on the Architecture via DNA Orientation. Binding an additional Fis molecule to the Fis−DNA complex yields other possibilities. To understand the effects of binding an additional Fis molecule on the relative orientation of two DNA molecules, we compared the free-energy profiles of the complex having a single Fis molecule with the profiles for complexes with two Fis molecules. Figure 5 illustrates the differences in free-energy profiles, highlighting the impact of varying Fis molecule stoichiometries on DNA orientation. In the single Fis system (Figure 5(A)), the free-energy surface shows a dominant population corresponding to an orthogonal (90°) orientation of the DNA molecules, labeled 1. In contrast, the two Fis systems exhibit multiple populations (Figure 5(B)), indicating that various orientations now become possible for the DNA segments (90, 60, and 20°), labeled 1′, 2′, and 3′, respectively. These results highlight the role of the second Fis molecule in modulating the orientation angle between the DNA segments by imposing a geometric restraint on the ends of each DNA segment.

To further analyze the stability of these intermediates, we assessed the free-energy barriers separating the distinct populations labeled 1′, 2′, and 3′ in the two Fis system. The orthogonal orientation (1′) remains relatively stable but is less populated than the intermediate (60°) orientation (2′), which has the lowest free energy and is the most favorable. The parallel configuration (3′) is less stable but still accessible, suggesting that the second Fis molecule enables a broader range of DNA orientations. Notably, the presence of the second Fis molecule shortens the distance between the two DNA molecules, as evident in the free-energy profiles, thereby enhancing the stability of nonorthogonal orientations (2′ and 3′). This effect likely results from the geometric restraints imposed by the second Fis molecule, which promotes closer interactions between the DNA segments. This diversification of orientations facilitates dynamic changes in the architecture, which are crucial in vivo for intersegment transfer.

3. DISCUSSION

3.1. Intersegment Transfer Process Can Be Described by Three-State Kinetics. We see that intersegment transfer of the Fis protein involves several intermediates, as identified from our free-energy landscape analysis. To gain deeper insight, we mapped these intermediates into a well-defined three-state kinetic model and estimated the corresponding rates. Figure 2B proposes a potential kinetic scheme for Fis protein intersegment transfer. The first intermediate, B_1, represents the fully bound state, where both anchors of the Fis protein are engaged with a single DNA molecule. The second intermediate, I, is a partially bound state where one anchor of the Fis protein remains bound to one DNA molecule, while the other anchor interacts with the second DNA molecule, forming a bridge-like configuration. The final intermediate, B_2, corresponds to the fully bound state, where both anchors of the Fis protein are engaged with the second DNA molecule. The transitions from B_1 and B_2 to intermediate state I are DNA-facilitated dissociation steps proportional to DNA concentration, while transitions from I back to B_1 or B_2 depend only on the concentration of the intermediate. Because the two DNA segments are equivalent, the corresponding kinetic coefficients are equal ($k_1 = k\_2$, $k_2 = k\_1$). Although alternative descriptions have been suggested by others,[18] our analysis shows that all of the proposed mechanisms are kinetically equivalent when the intermediate state is unstable. One alternative proposed mechanism introduces an additional intermediate state between B_1 and I, in which one chain of the Fis protein remains bound to one DNA while the other chain dissociates completely. This intermediate, however, is energetically unfavorable compared to the partially bound species (I) observed in our mechanism. This additional intermediate acts much like a transition state so that the two mechanisms are kinetically equivalent, as detailed in the Supporting Information. Thus, the intersegment transfer process effectively follows a three-state kinetic model:

$$B_1 \underset{k_{-1}}{\overset{k_1 c}{\rightleftharpoons}} I \underset{k_{-2} c}{\overset{k_2}{\rightleftharpoons}} B_2 \tag{1}$$

Experimental data have shown that the average dissociation time of the Fis protein depends on DNA segment concentration (eq S9). By calculating the mean first-passage time from one binding state (B_1) to another (B_2) and applying the relationships between kinetic coefficients (eq S8), we estimated the rate constants using the values from experiments.[18,32] Specifically, k_1 is estimated to range from 0.0078 to 0.0093 $(\mathrm{M{\cdot}s})^{-1}$, while k_{-1} ranges from 2.096×10^4 to 2.407×10^4 s^{-1}.

We can also use Kramers' theory to obtain rate coefficients from the free-energy profiles derived from our simulations.[19,20] Previous studies have established the dynamical parameters in Kramers' theory for the Fis system using our force field (eq S12). Using the free-energy profile constructed through our simulations (eq S11) yields a value for the rate constant k_1 of 0.0085 $(\mathrm{M{\cdot}s})^{-1}$, while k_{-1} turns out to be 2.22×10^4 s^{-1}. We see these simulation-derived rate constants closely align with experimental data, providing quantitative validation of our hypothesis.

3.2. DNA Orientational Effects on the Transfer Process in the Fis Protein−DNA Complex Architecture. Previously, Levy and co-workers proposed a "Monkey-bar" mechanism for the Pax6 protein in which intersegment transfer between two DNA molecules is facilitated by two distinct protein domains: a structured domain and a disordered tail.[33,34] The disordered tail enhances the efficiency of the DNA search process and supports the transfer between DNA segments. In contrast to the key involvement of the disordered segment, the Fis protein employs its structured anchor to engage with DNA during intersegment transfer. The architecture of the Fis protein−DNA complex still plays a functionally analogous role to that of the disordered tail by facilitating DNA interactions, but its rigidity simultaneously imposes orientational constraints on the DNA molecules. These orientational effects may provide conformational selectivity, favoring certain transfer pathways over others in the assembly of larger complexes in vivo. Similar mechanical coupling between Fis-mediated DNA architecture and its dynamic regulatory functions has been observed in site-specific recombination, where DNA supercoiling and enhancer-bound Fis impose rotational constraints critical for functional transitions.[10]

Different configurational states mediate intersegment transfer pathways in distinct ways. The parallel orientation of DNA molecules favors the formation of the major−minor groove species due to its specific DNA orientational effects. This intermediate then transitions into the major−major groove

https://doi.org/10.1021/jacs.5c09262
J. Am. Chem. Soc. 2025, 147, 30277−30286

species to complete the intersegment transfer, as illustrated in Figure 6 (Pathway 1). This stepwise route is kinetically more

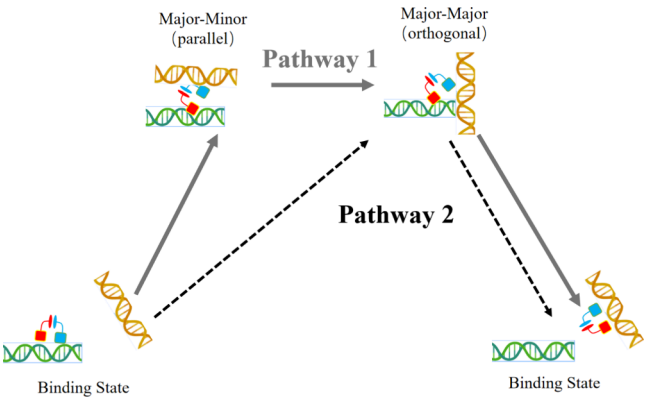

Figure 6. A schematic diagram of the kinetic pathway of intersegment transfer of the Fis molecule on DNA. The pathway is illustrated in terms of the switching between major/minor grooves along DNA molecules (parallel vs orthogonal). In this process, one anchor of the Fis protein remains on the major groove of one DNA, while the other anchor of the Fis protein searches for another DNA to complete the transfer process. In pathway 1 (parallel DNAs), the intersegment transfer is carried out through major grooves on both DNAs, while in pathway 2 (orthogonal DNAs), the major−minor intermediate is formed first followed by the major−major complex to complete the entire transfer process.

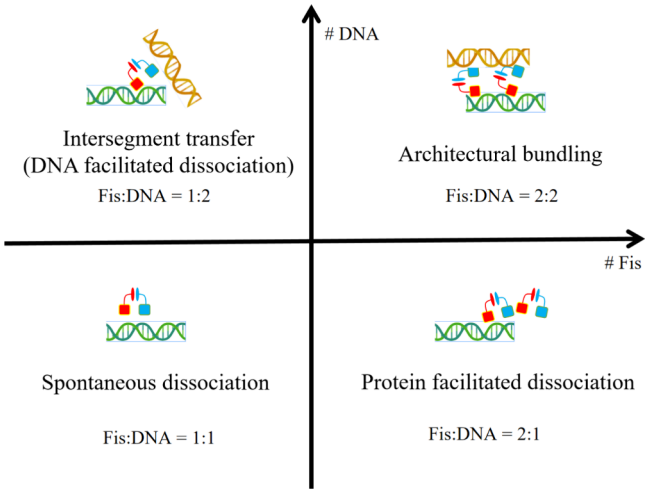

Figure 7. Schematic diagram of the stoichiometric effect in the Fis−DNA system. Lower left) Fis protein with one DNA molecule illustrating spontaneous dissociation. Lower right) Two Fis proteins with one DNA molecule demonstrating protein-facilitated dissociation. Upper left) One Fis protein with two DNA molecules showing intersegment transfer (DNA-facilitated dissociation). Upper right) Two Fis proteins with two DNA molecules depicting architectural bundling.

favorable than a direct transition through the major−major groove species, which dominates when the DNA molecules adopt an orthogonal configuration (Pathway 2).

Given the influence of DNA orientational effects, the orthogonal configuration is generally preferred as it stabilizes the major−major groove species when the DNA orientation is unconstrained. In summary, the orientational constraints imposed by both the Fis−DNA complex and the DNA molecules themselves play a crucial role in guiding transition pathways and shaping the architectural landscape of the Fis protein−DNA complexes.

3.3. Concentration Effects on Fis−DNA Systems. The behavior of the Fis−DNA complex is complex, particularly when considering how different concentration ratios of Fis protein to DNA are encountered at different stages of the cell's life. Previous studies have demonstrated that the Fis protein can spontaneously dissociate from DNA (upper left in Figure 7).[19] Both experiments and simulations indicate that the presence of a second Fis protein however facilitates this dissociation process[18,20] (upper right). Furthermore, the present work shows that a second DNA segment will also aid in the dissociation of the Fis protein (lower left), a finding corroborated by experimental results.[18] The presence of a second Fis protein and the second DNA segment alters the preferred dissociation pathway through their architectural bundling (lower right). Given the complexity introduced by the different stoichiometries, the kinetics of Fis protein dissociation in vivo vary with changes in the relative concentrations of Fis protein and DNA.

The stoichiometric effects of Fis molecules in different molecularity complexes have several potential implications under cellular conditions. First, the stabilization of multiple DNA orientations by the second Fis molecule may contribute to its role in gene regulation. By the modulation of DNA orientation, Fis could influence the accessibility of the necessary specific regulatory regions that must be read in sequence or enhance interactions with other proteins involved in transcription, replication, or recombination. The flexibility afforded by the two Fis systems might enable a more adaptive response to cellular signals or environmental changes. We also see that there is a clear Fis-facilitated screw-like motion of DNA segments in the assembly, suggesting that the supercoiling of DNA may be critical to Fis regulation in vivo.

Second, the kinetic control of intersegment transfer may benefit from the geometric restraint imposed by the two Fis molecules. The ability to stabilize intermediate states such as architectural protein−DNA complexes (2′ or 3′ shown in Figure 5D) could facilitate efficient transitions between DNA segments, reducing the time required for proteins to locate their target sequences on the genome. This is particularly relevant for processes such as transcription factor binding or DNA repair, where speed and precision are critical.

Finally, the architectural roles of Fis molecules under different cellular conditions might extend to maintaining higher-order chromosomal structures. The modulation of DNA orientation could contribute to nucleoid organization, allowing for the compaction and organization of genetic material without compromising the accessibility. By providing a structural scaffold, the second Fis molecule may enhance the mechanical stability of DNA during dynamic processes, such as chromosome segregation or replication.

In summary, the presence of a second Fis molecule not only broadens the range of DNA orientations but also reduces the distance between the two DNA molecules, thereby stabilizing specific intermediates that may play crucial roles in gene regulation, kinetically controlled processes, and DNA organization. These findings underscore how changes in Fis stoichiometry can induce emergent effects, such as enhanced DNA compaction and stabilization of regulatory intermediates under cellular conditions by influencing DNA architecture and function. The length of the DNA segments can influence both

https://doi.org/10.1021/jacs.5c09262
J. Am. Chem. Soc. 2025, 147, 30277−30286

the thermodynamics and the kinetics of the intersegment transfer process, which we plan to investigate in future studies.

4. METHODS

4.1. Coarse-Grained Model for Protein and DNA. All simulations in this work were performed by a hybrid model called the AWSEM/3SPN.2C model. In this hybrid model, the protein is modeled by AWSEM (associative memory, water-mediated, structure, and energy model), a predictive coarse-grained protein-folding force field. And the DNA is modeled using the 3SPN.2C force field. This hybrid model has already succeeded in various protein−DNA systems.[19,20,30,31,35] The details of the calibration of protein−DNA interactions and the calculation of free-energy landscapes can be found in previous works.[19] We use the crystal structure of Fis (PDB ID: 3IV5)[3] and the binding sequence (AAATTTGTTTGAATTTTG-AGCAAATTT) as the starting points in our simulations.

4.2. Simulation Details Using the AWSEM/3SPN.2C Model. In this work, all umbrella sampling simulations for the Fis−DNA system were performed using LAMMPS (large-scale atomic/molecular massively parallel simulator) at 300 K for 6 million steps.[36,37] In the earlier paper, 6 million steps corresponds to around 30 μs in laboratory time.[30] This duration is sufficient to ensure convergence in the sampling of the entire system. To investigate the binding process phenomenon, we conducted one set of simulations involving one Fis protein and two DNA molecules. The simulations utilized the electrostatic interaction between the Fis protein and a DNA sequence as a biased coordinate, employing 25 windows. These windows were employed by varying the electrostatic interaction between the Fis protein and one DNA, ranging from −1 to −25 kcal/mol.

To examine the influence of the relative geometry of DNA molecules, we conducted two sets of simulations. One set constrained the two DNA molecules in a parallel orientation, while the other set fixed the two DNA molecules in an orthogonal orientation. The center-of-mass distance between the two DNA molecules was maintained at 50 Å. Both sets of simulations involved one Fis protein and two DNA molecules, using the electrostatic interactions between the Fis protein and DNA sequences as a biased coordinate. These interactions ranged from −1 to −30 kcal/mol across 30 windows. Additionally, each set of simulations included three different initial relative positions of the Fis protein and DNA: 1) Fis on DNA1, 2) Fis on DNA2, and 3) Fis between DNA1 and DNA2. The results were analyzed by averaging the data from these simulations.

We conducted two additional sets of simulations to further investigate the binding process. The first set included one Fis protein and two DNA molecules, differing from the previous set by not applying any constraints on the orientation and distance between the two DNA molecules. The second set included two Fis proteins and two DNA molecules, without any constraints on the system. These sets utilized the electrostatic interactions between one Fis protein and two DNA molecules as a biased coordinate across 30 windows. The simulations for each window were conducted by varying the electrostatic interactions between one Fis protein and the two DNA sequences, ranging from −1 to −30 kcal/mol.

4.3. Geometric Parameters of Fis−DNA Systems. Figure 2 illustrates the details of the Fis protein−DNA complex. The anchor of chain A is colored red, while the anchor of chain B is colored blue. Notably, the major grooves and minor grooves do not change during the simulations in our systems. The types of contacts are identified by the number and categories of binding base pairs.

■ ASSOCIATED CONTENT

Data Availability Statement

The raw input files, data from simulation, data from analysis in this work, and analysis codes in this work have been deposited in GitHub:https://github.com/chemlover/Fis_Intersegment_Transfer. The AWSEM-3SPN2 codes in this work have been deposited in GitHub:https://github.com/adavtyan/awsemmd.

Supporting Information

The Supporting Information is available free of charge at https://pubs.acs.org/doi/10.1021/jacs.5c09262.

Descriptions of kinetic models, groove specificity, and stoichiometry effect of the intersegment transfer process (PDF)

Movie of the intersegment transfer process (MP4)

PDB file of the intersegment transfer process (PDB)

■ AUTHOR INFORMATION

Corresponding Authors

Xun Chen − *Department of Medicinal Chemistry, National Vaccine Innovation Platform, School of Pharmacy, Nanjing Medical University, Nanjing, Jiangsu 211166, China; Center for Theoretical Biological Physics, Houston, Texas 77005, United States;* orcid.org/0000-0002-0601-8397; Email: chenxun@njmu.edu.cn

Yaakov Levy − *Weizmann Institute of Science, Rehovot 76100, Israel;* orcid.org/0000-0002-9929-973X; Email: koby.levy@weizmann.ac.il

Min-Yeh Tsai − *Department of Chemistry and Biochemistry, National Chung Cheng University, Minhsiung, Chiayi 621301, Taiwan; Center for Nano Bio-Detection, National Chung Cheng University, Minhsiung, Chiayi 621301, Taiwan;* orcid.org/0000-0002-6275-0312; Email: myt@ccu.edu.tw

Peter G. Wolynes − *Center for Theoretical Biological Physics, Houston, Texas 77005, United States; Department of Chemistry, Rice University, Houston, Texas 77005, United States; Department of Biosciences, Rice University, Houston, Texas 77005, United States;* orcid.org/0000-0001-7975-9287; Phone: (713) 348-4101; Email: pwolynes@rice.edu

Authors

Shikai Jin − *Center for Theoretical Biological Physics, Houston, Texas 77005, United States;* orcid.org/0000-0001-9525-4166

Cheng-Han Liu − *Department of Chemistry and Biochemistry, National Chung Cheng University, Minhsiung, Chiayi 621301, Taiwan; Center for Nano Bio-Detection, National Chung Cheng University, Minhsiung, Chiayi 621301, Taiwan*

Complete contact information is available at: https://pubs.acs.org/10.1021/jacs.5c09262

Notes

The authors declare no competing financial interest.

■ ACKNOWLEDGMENTS

This work is funded by the G. Harold & Leila Y. Mathers Charitable Foundation primary award no. 30086506 (P.G.W. and Komives). It is also supported by the Center for Theoretical Biological Physics, sponsored by NSF grant PHY-2019745. Additionally, we wish to recognize the D. R. Bullard Welch Chair at Rice University, grant C-0016 (to P.G.W.). We thank the Data Analysis and Visualization Cyberinfrastructure funded by National Science Foundation grant OCI-0959097. M.-Y.T. would like to thank the National Science and Technology Council (NSTC), Taiwan for supporting this work (grant no. NSTC-113-2628-M-194-001-MY3). M.-Y.T. also acknowledges support from the National Center for Theoretical Sciences (NCTS), Physics Division,

Taiwan (Thematic Group on Nanoscale Physics and Chemistry). X.C. would like to thank the Nanjing Medical University (grant no. NMUR 2024007) for supporting this work.

REFERENCES

(1) Bradley, M. D.; Beach, M. B.; de Koning, A. J.; Pratt, T. S.; Osuna, R. Effects of Fis on Escherichia coli gene expression during different growth stages. *Microbiology* **2007**, *153*, 2922−2940.
(2) Hager, G. L.; McNally, J. G.; Misteli, T. Transcription dynamics. *Molecular cell* **2009**, *35*, 741−753.
(3) Stella, S.; Cascio, D.; Johnson, R. C. The shape of the DNA minor groove directs binding by the DNA-bending protein Fis. *Genes & development* **2010**, *24*, 814−826.
(4) Swinger, K. K.; Lemberg, K. M.; Zhang, Y.; Rice, P. A. Flexible DNA bending in HU-DNA cocrystal structures. *EMBO Journal* **2003**, *22*, 3749−3760.
(5) Hirvonen, C. A.; Ross, W.; Wozniak, C. E.; Marasco, E.; Anthony, J. R.; Aiyar, S. E.; Newburn, V. H.; Gourse, R. L. Contributions of UP elements and the transcription factor FIS to expression from the seven rrn P1 promoters in Escherichia coli. *Journal of bacteriology* **2001**, *183*, 6305−6314.
(6) Travers, A.; Schneider, R.; Muskhelishvili, G. DNA supercoiling and transcription in Escherichia coli: The FIS connection. *Biochimie* **2001**, *83*, 213−217.
(7) Muskhelishvili, G.; Buckle, M.; Heumann, H.; Kahmann, R.; Travers, A. FIS activates sequential steps during transcription initiation at a stable RNA promoter. *EMBO journal* **1997**, *16*, 3655−3665.
(8) Finkel, S.; Johnson, R. The Fis protein: it's not just for DNA inversion anymore. *Molecular microbiology* **1992**, *6*, 3257−3265.
(9) Roilides, E.; Simitsopoulou, M.; Katragkou, A.; Walsh, T. J. How biofilms evade host defenses. *Microbiology spectrum* **2015**, *3*, 3−3.
(10) Dhar, G.; Heiss, J. K.; Johnson, R. C. Mechanical constraints on Hin subunit rotation imposed by the Fis/enhancer system and DNA supercoiling during site-specific recombination. *Molecular cell* **2009**, *34*, 746−759.
(11) Heichman, K. A.; Johnson, R. C. The Hin invertasome: protein-mediated joining of distant recombination sites at the enhancer. *Science* **1990**, *249*, 511−517.
(12) Bruist, M. F.; Glasgow, A. C.; Johnson, R. C.; Simon, M. I. Fis binding to the recombinational enhancer of the Hin DNA inversion system. *Genes & development* **1987**, *1*, 762−772.
(13) Nasser, W.; Rochman, M.; Muskhelishvili, G. Transcriptional regulation of fis operon involves a module of multiple coupled promoters. *EMBO journal* **2002**, *21*, 715−724.
(14) Gille, H.; Egan, J. B.; Roth, A.; Messer, W. The FIS protein binds and bends the origin of chromosomal DNA replication, oriC, of Escherichia coli. *Nucleic acids research* **1991**, *19*, 4167−4172.
(15) Graham, J. S.; Johnson, R. C.; Marko, J. F. Concentration-dependent exchange accelerates turnover of proteins bound to double-stranded DNA. *Nucleic acids research* **2011**, *39*, 2249−2259.
(16) Jeong, J.; Le, T. T.; Kim, H. D. Single-molecule fluorescence studies on DNA looping. *Methods* **2016**, *105*, 34−43.
(17) Erbaş, A.; Marko, J. F. How do DNA-bound proteins leave their binding sites? The role of facilitated dissociation. *Curr. Opin. Chem. Biol.* **2019**, *53*, 118−124.
(18) Giuntoli, R. D.; Linzer, N. B.; Banigan, E. J.; Sing, C. E.; De La Cruz, M. O.; Graham, J. S.; Johnson, R. C.; Marko, J. F. DNA-segment-facilitated dissociation of Fis and NHP6A from DNA detected via single-molecule mechanical response. *Journal of molecular biology* **2015**, *427*, 3123−3136.
(19) Tsai, M.-Y.; Zhang, B.; Zheng, W.; Wolynes, P. G. Molecular mechanism of facilitated dissociation of Fis protein from DNA. *J. Am. Chem. Soc.* **2016**, *138*, 13497−13500.
(20) Tsai, M.-Y.; Zheng, W.; Chen, M.; Wolynes, P. G. Multiple binding configurations of Fis protein pairs on DNA: Facilitated dissociation versus cooperative dissociation. *J. Am. Chem. Soc.* **2019**, *141*, 18113−18126.
(21) Kamar, R. I.; Banigan, E. J.; Erbas, A.; Giuntoli, R. D.; De La Cruz, M. O.; Johnson, R. C.; Marko, J. F. Facilitated dissociation of transcription factors from single DNA binding sites. *Proc. Natl. Acad. Sci. U. S. A.* **2017**, *114*, E3251−E3257.
(22) Hadizadeh, N.; Johnson, R. C.; Marko, J. F. Facilitated dissociation of a nucleoid protein from the bacterial chromosome. *Journal of bacteriology* **2016**, *198*, 1735−1742.
(23) McCauley, M. J.; Rueter, E. M.; Rouzina, I.; Maher, L. J., III; Williams, M. C. Single-molecule kinetics reveal microscopic mechanism by which High-Mobility Group B proteins alter DNA flexibility. *Nucleic acids research* **2013**, *41*, 167−181.
(24) Joshi, C. P.; Panda, D.; Martell, D. J.; Andoy, N. M.; Chen, T.-Y.; Gaballa, A.; Helmann, J. D.; Chen, P. Direct substitution and assisted dissociation pathways for turning off transcription by a MerR-family metalloregulator. *Proc. Natl. Acad. Sci. U. S. A.* **2012**, *109*, 15121−15126.
(25) Mahmutovic, A.; Berg, O. G.; Elf, J. What matters for lac repressor search in vivo—sliding, hopping, intersegment transfer, crowding on DNA or recognition? *Nucleic acids research* **2015**, *43*, 3454−3464.
(26) Itoh, Y.; Murata, A.; Takahashi, S.; Kamagata, K. Intrinsically disordered domain of tumor suppressor p53 facilitates target search by ultrafast transfer between different DNA strands. *Nucleic acids research* **2018**, *46*, 7261−7269.
(27) Menetski, J. P.; Kowalczykowski, S. C. Transfer of recA protein from one polynucleotide to another. Kinetic evidence for a ternary intermediate during the transfer reaction. *J. Biol. Chem.* **1987**, *262*, 2085−2092.
(28) Kunzelmann, S.; Morris, C.; Chavda, A. P.; Eccleston, J. F.; Webb, M. R. Mechanism of interaction between single-stranded DNA binding protein and DNA. *Biochemistry* **2010**, *49*, 843−852.
(29) Chen, X.; Lu, W.; Tsai, M.-Y.; Jin, S.; Wolynes, P. G. Exploring the folding energy landscapes of heme proteins using a hybrid AWSEM-heme model. *Journal of Biological Physics* **2022**, *48*, 37.
(30) Potoyan, D. A.; Zheng, W.; Komives, E. A.; Wolynes, P. G. Molecular stripping in the NF-κB/IκB/DNA genetic regulatory network. *Proc. Natl. Acad. Sci. U. S. A.* **2016**, *113*, 110−115.
(31) Chen, X.; Tsai, M.-Y.; Wolynes, P. G. The role of charge density coupled DNA bending in transcription factor sequence binding specificity: a generic mechanism for indirect readout. *J. Am. Chem. Soc.* **2022**, *144*, 1835−1845.
(32) Ninio, J. Alternative to the steady-state method: derivation of reaction rates from first-passage times and pathway probabilities. *Proc. Natl. Acad. Sci. U. S. A.* **1987**, *84*, 663−667.
(33) Vuzman, D.; Levy, Y. DNA search efficiency is modulated by charge composition and distribution in the intrinsically disordered tail. *Proc. Natl. Acad. Sci. U. S. A.* **2010**, *107*, 21004−21009.
(34) Vuzman, D.; Azia, A.; Levy, Y. Searching DNA via a "Monkey Bar" mechanism: the significance of disordered tails. *Journal of molecular biology* **2010**, *396*, 674−684.
(35) Chen, X.; Jin, S.; Chen, M.; Bueno, C.; Wolynes, P. G. The marionette mechanism of domain-domain communication in the antagonist, agonist, and coactivator responses of the estrogen receptor. *Proc. Natl. Acad. Sci. U. S. A.* **2023**, *120*, e2216906120.
(36) Davtyan, A.; Schafer, N. P.; Zheng, W.; Clementi, C.; Wolynes, P. G.; Papoian, G. A. AWSEM-MD: protein structure prediction using coarse-grained physical potentials and bioinformatically based local structure biasing. *J. Phys. Chem. B* **2012**, *116*, 8494−8503.
(37) Freeman, G. S.; Hinckley, D. M.; Lequieu, J. P.; Whitmer, J. K.; De Pablo, J. J. Coarse-grained modeling of DNA curvature. *J. Chem. Phys.* **2014**, *141*, 165103.

https://doi.org/10.1021/jacs.5c09262
J. Am. Chem. Soc. 2025, 147, 30277−30286